
123D: Unifying Multi-Modal Autonomous Driving Data at Scale

Daniel Dauner^{1,2} Valentin Charrat⁴ Bastian Berle² Tianyu Li⁵
Long Nguyen^{1,2} Jiabao Wang⁶ Changhui Jing⁵ Maximilian Igl³
Holger Caesar⁷ Boris Ivanovic³ Yiyi Liao⁶ Andreas Geiger¹ Kashyap Chitta^{1,3}
¹KE:SAI ²University of Tübingen, Tübingen AI Center ³NVIDIA Research
⁴Valeo Brain ⁵OpenDriveLab at Shanghai Innovation Institute ⁶Zhejiang University
⁷Delft University of Technology

Abstract

The pursuit of autonomous driving has produced one of the richest sensor data collections in all of robotics. However, its scale and diversity remain largely untapped. Each dataset adopts different 2D and 3D modalities, such as cameras, lidar, ego states, annotations, traffic lights, and HD maps, with different rates and synchronization schemes. They come in fragmented formats requiring complex dependencies that cannot natively coexist in the same development environment. Further, major inconsistencies in annotation conventions prevent training or measuring generalization across multiple datasets. We present 123D, an open-source framework that unifies such multi-modal driving data through a single API. To handle synchronization, we store each modality as an independent timestamped event stream with no prescribed rate, enabling synchronous or asynchronous access across arbitrary datasets. Using 123D, we consolidate eight real-world driving datasets spanning 3,300 hours and 90,000 kilometers, together with a synthetic dataset with configurable collection scripts, and provide tools for data analysis and visualization. We conduct a systematic study comparing annotation statistics and assessing each dataset’s pose and calibration accuracy. Further, we showcase two applications 123D enables: cross-dataset 3D object detection transfer and reinforcement learning for planning, and offer recommendations for future directions. Code and documentation are available at <https://github.com/kesai-labs/py123d>.

1 Introduction

Progress in autonomous driving research is strongly tied to dataset releases. Every milestone in the field, from modular perception [25, 6, 56], behavior prediction [10, 21, 29], to end-to-end driving [68, 51], has introduced new datasets, expanding a still-growing collection of driving recordings.

This collection is rarely studied as a whole. Instead, models are typically trained and evaluated on splits of the same dataset. Each dataset is tied to specific biases, e.g., a single sensor configuration, a single vehicle type, a handful of cities, and a particular collection period [61, 48]. It is likely infeasible to establish generalizable driving intelligence via training on any single dataset with such inherent biases. Re-collecting data for each deployment is also not a workable approach: sensor stacks, operating domains, and demographic coverage all shift over time [65, 63, 64, 52], and re-collection at sufficient scale each time requirements change is prohibitively expensive. Several questions arise on how to go forward: how to curate what already exists, how to scale heterogeneous datasets jointly, and how to combine real with synthetic data. None of these can be addressed one dataset at a time.

Despite the potential societal impact and research effort invested into autonomous driving, the community so far has limited infrastructure for managing data. Natural language processing consolidates around shared corpora and libraries (e.g., Common Crawl [23], Hugging Face Datasets [40]) that make systematic evaluation routine and, in turn, have enabled scaling of large language models. Gen-

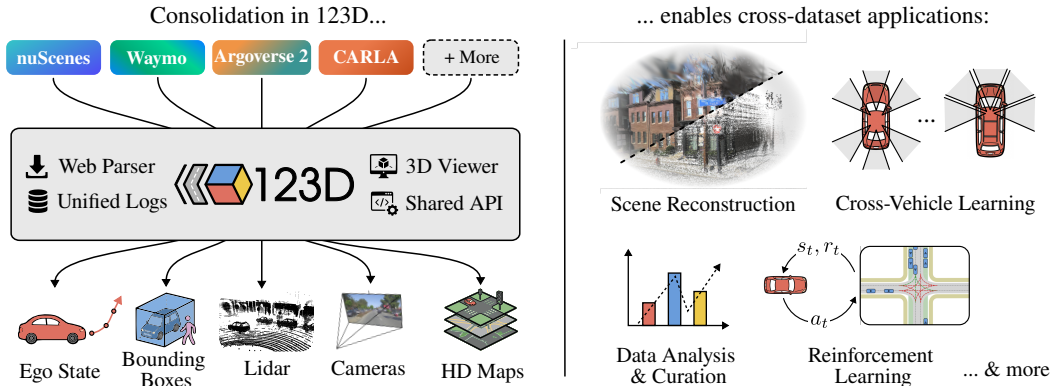


Figure 1: 123D. An open-source toolkit to consolidate fragmented driving data through a unified format for modalities such as annotations, sensors, and HD maps. By overcoming this fragmentation, 123D enables a wide range of cross-dataset applications and research directions, including scene reconstruction, cross-vehicle learning, and reinforcement-learning-based planning.

eral robotics has done the same with LeRobot [5] and Open X-Embodiment [14], where unified access to data from dozens of robotic platforms has already produced generalist policies and demonstrable cross-embodiment transfer [2]. The consistent pattern across fields is that consolidation precedes scale, and that scale, when paired with sufficient diversity, changes what the field achieves [4].

In this paper, we establish such consolidation through 123D: *one* unified interface for 2D and 3D driving data (Fig. 1). We provide a log format handling arbitrary frequencies and synchronization schemes, alongside a principled approach to unifying conventions. This allows us to populate 123D with eight established datasets, such as nuScenes [6], the Waymo Open Dataset [56, 21], and Argoverse 2 [66], and contribute a synthetic dataset collected in CARLA [20]. Due to the variance across these datasets, 123D involves a substantial one-time initial engineering effort (Sec. 3.1), thereby significantly simplifying the addition of new datasets to the collection. Our contributions are: (1) We open-source `py123d`, a Python library and autonomous driving toolkit providing conversion, unified access, and visualization for the above format and datasets. (2) We conduct a systematic cross-dataset analysis of annotation, pose, and calibration quality that informs dataset understanding and guides curation across heterogeneous sources. (3) We demonstrate cross-dataset 3D object detection and reinforcement-learning-based planning, where we provide empirical evidence supporting the premise that training on heterogeneous datasets assists both in-domain and cross-domain generalization.

2 Related Work

Driving Datasets. Since KITTI [25] laid the foundations with stereo camera and lidar data, public driving datasets have grown considerably in scale and sensor coverage. Each release is typically introduced for a specific set of benchmark tasks, e.g., perception [6, 56, 46], motion forecasting [10, 66, 21], data-driven planning [35], or end-to-end driving on either real [68] or synthetic data [55, 34, 50]. Often, these data sources are shaped by task and engineering conventions of the organization that released them. Moreover, several datasets have been repurposed to new emergent tasks as the field progresses [30, 45, 55, 18, 42, 7], demonstrating the need for tooling that handles general driving recordings uniformly. In this work, we provide such tooling capable of handling diverse datasets to support research on a wide variety of autonomous driving tasks.

Cross-Dataset Frameworks. The robotics community has consolidated around shared data ecosystems such as LeRobot [5] and Open X-Embodiment [14], which accelerate progress by providing unified formats and tooling for training across heterogeneous platforms. The driving community has pursued similar approaches, but each effort is purpose-built for a narrow family of tasks: agent trajectories and maps are consolidated for motion prediction and planning simulation [33, 41, 43, 22], point clouds or images for 3D object detection [15, 57], or raw sensor data for novel-view synthesis and scene reconstruction [58, 12]. However, each framework makes task-specific simplifications that make combining such tools challenging. For instance, trajdata [33] and ScenarioNet [41] discard all sensors and resample logs onto a single fixed rate, while MMDetection3D [15] and OpenPCDet [57] retain only detection-relevant subsets of each dataset. OmniRe [12] preserves multi-camera and lidar

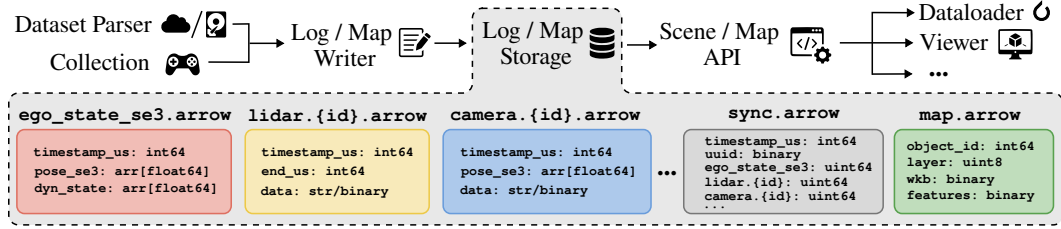


Figure 2: Architecture. We parse existing datasets from cloud/local storage, or collect data in simulation that we write to our unified Apache Arrow [24] log format (Sec. 3.1). The scene and map API enable access to logs, and can be passed to a dataloader, viewer, or other application (Sec. 3.2).

observations, but with fixed per-dataset sample rates at pre-processing time and provides no map or traffic-light abstraction. Recently, OmniLiDAR [38] aggregates 12 datasets, but only for lidar point clouds. In this work, we instead expose raw sensor data, agent annotations, maps, and ego states as modular, independent streams under a shared API, without enforcing fixed rates or episode lengths. We demonstrate 123D’s generality on each of the task families above (i.e., planning simulation, 3D detection, and scene reconstruction) for a heterogeneous collection of datasets.

3 The 123D Framework

Existing driving datasets differ widely in sensor configurations, coordinate conventions, label taxonomies, modality frequencies, and map representations. To address this heterogeneity, we develop `py123d`, an open-source Python package (Apache 2.0) that parses disparate sources into a uniform log and map format (Sec. 3.1) and provides common data access and tooling on top of it (Sec. 3.2). In the following, we describe the key challenges encountered and how our framework addresses them.

3.1 Data Format & Conversion

Source Formats & Dependencies. Each dataset comes with a different file layout, often with optional or outdated dependencies that cannot coexist in a single environment. We encapsulate all dataset-specific logic in a *dataset parser* that reads the source data, converts it to the 123D datatypes and conventions, and passes the unified log and map content to a shared *log writer/map writer* (Fig. 2). Each parser operates on a local copy of the source dataset. As most driving dataset providers permit scripted downloads [6, 56, 66, 67, 21, 35, 51, 53, 50], our parser fetches the raw data directly, so that a single terminal command both downloads and converts the dataset into 123D files.

Heterogeneous Modalities at Varying Frequencies. Recordings may be of variable durations even within a single dataset, capturing modalities at vastly different rates. Some provide data synchronously at shared keyframes, while others are recorded asynchronously as independent events. To handle this inconsistency, we represent all continuous driving recordings as a *log*: a directory of Apache Arrow IPC files [24], with one dataframe of timestamped events per modality (Fig. 2). A separate *sync table* records, for each synchronized frame, the corresponding row index in every modality’s dataframe, so that cross-modal alignment is precomputed once and available as a direct lookup at access time. The sync table is configurable: it can preserve the source dataset’s original keyframes, operate given a chosen reference modality, and optionally resample to a target rate. Since modalities remain independent event streams in storage, the access layer can optionally bypass the sync table and retrieve data at arbitrary timestamps. Moreover, static metadata (e.g., vehicle extent, sensor calibration) is embedded independently in each file’s Arrow schema. 123D supports a broad set of modalities, including ego-states, 3D bounding boxes, traffic light states, user-defined custom datatypes, lidar point clouds, and camera images with multiple projection models.

External vs. Self-contained Logs. Raw sensor data, such as high-resolution images and point clouds, typically dominates a dataset’s storage footprint. To avoid data duplication if a dataset is stored locally, our format defaults to an *external* approach, such as storing relative file paths. However, our format may also operate *self-contained*, where sensor data is serialized directly into the log files. A self-contained log is particularly beneficial for portability, parsing a dataset from cloud storage, or when large numbers of small files impose strain on a storage system [1]. We support various compression codecs (e.g., JPEG, PNG, MP4 for camera data; Draco, LAZ, or IPC binaries for

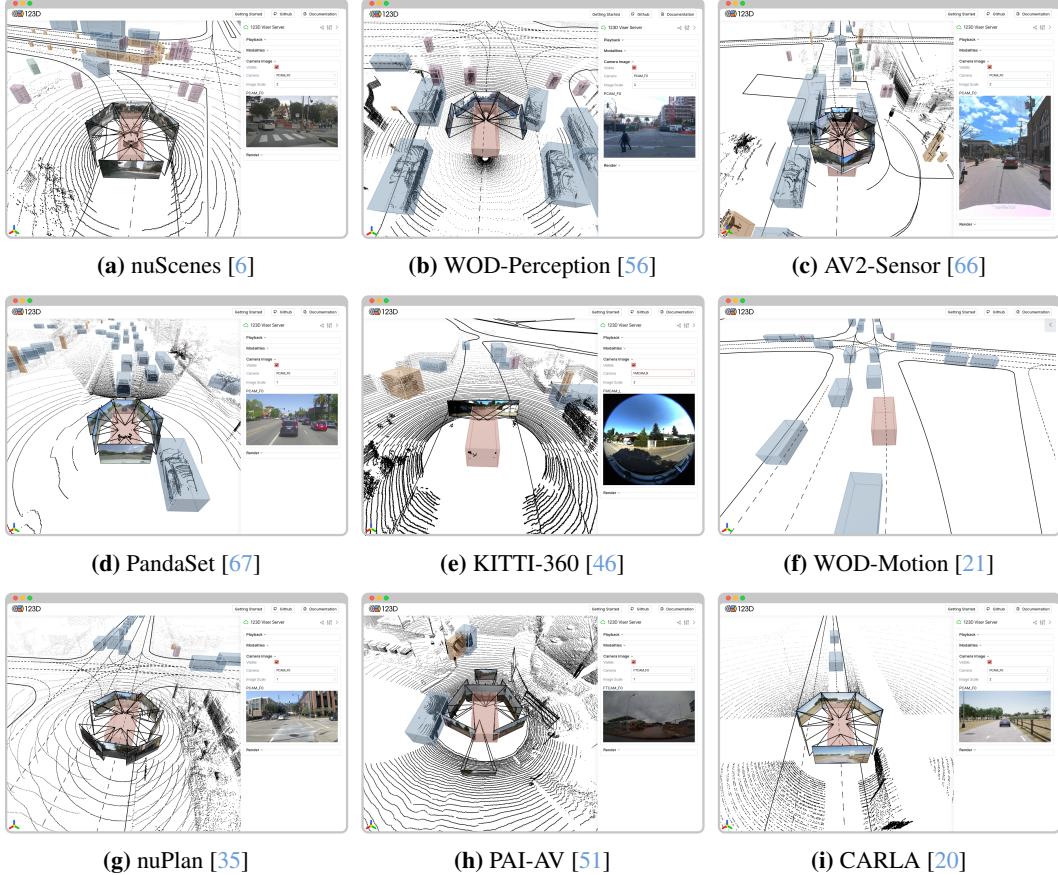


Figure 3: 3D Viewer. Analyzing driving recordings requires frequent visual inspections. We show visualizations of supported datasets in 3a-3i from our interactive 3D viewer based on Viser [71].

lidar point clouds), to remain configurable along trade-offs between storage size and access latency. Importantly, sensor data access returns unified representations agnostic to the storage choice.

Structural variance in HD maps. HD map representations across datasets differ in semantic granularity, spatial coverage (city-wide vs. per-log), or dimensionality (3D vs. 2D). We define a vector-based map representation that covers the superset of objects encountered across supported datasets, distinguishing between *polygon* and *polyline* objects. Polygon objects include `Lane` (with centerline, boundaries, speed limits, and neighbor references), `LaneGroup` (a collection of co-directional lanes forming a graph), `Intersection` (junctions linking internal lane groups), as well as `Crosswalk`, `Carpark`, `Walkway`, `GenericDrivable`, `StopZone`, and `SpeedBump` each with 2D/3D polygon and triangle mesh attributes. Polyline objects include `RoadEdge` (drivable/non-drivable boundaries) and `RoadLine` (semantic markings such as solid white or dashed yellow lines). All map elements are stored in a single Arrow IPC file with encoded object features and their geometry represented as Well-Known Binary (WKB) representations [31]. This representation enables fast bulk reads and initialization of a Sort-Tile-Recursive (STR) tree [39] used during map queries. Maps can reside within a specific log directory or dataset directory when shared across multiple logs, as is common with city-wide maps.

Inconsistent Labels & Conventions. Label taxonomies across datasets may not fully align due to differences in the annotation guidelines. Rather than imposing a single taxonomy, our framework preserves original labels and provides deferred mappings to common semantic categories. Coordinate conventions also differ across datasets, requiring careful alignment when combining data from multiple sources. To remove this burden, we enforce standardized conventions across all converted datasets: the *Body Frame* for the ego vehicle pose and bounding boxes follows ISO 8855 [32] (x : forward, y : left, z : up; e.g., [6, 56, 66]); the *Camera Frame* uses the OpenCV convention [3] (x : right, y : down, z : forward; e.g., [6, 66, 46]); and global coordinates follow the source dataset’s native definition. Since the ego-pose origin varies between datasets (e.g., ground plane [51], or IMU

position [46]), we provide transformations, partially inferred from the vehicle model, to both the rear-axle and vehicle center to support tasks such as motion planning and collision checking.

3.2 Data Access & Visualization

Scene API. Common workflows with driving data involve managing sub-sequences of recordings, history and future time windows, or resampling between source and target frequencies. Our framework provides a *Scene API* that makes these patterns declarative: the user specifies the desired datasets, reference frequency, and required modalities, and receives lightweight scene objects that serve as views into the underlying driving logs. To instantiate a large number of scenes (e.g., within a dataloader), we keep memory usage proportional to what is accessed rather than what is indexed. Scenes store log and index references internally, and modalities are loaded on demand through a shared, least-recently-used (LRU) cache of memory-mapped log files. The API supports multiple access modes: modalities can be retrieved at a synchronized iteration, queried asynchronously around a timestamp (i.e., with exact, nearest, forward, or backward matching), or within a time window. This is particularly useful when modalities have different native frequencies, e.g., when pairing each lidar sweep with the nearest camera frame at the camera’s native rate.

Map API. HD-maps require specialized data access, such as nearest-neighbor or intersection queries over map objects, which become expensive when applied naively to large, city-wide maps. We provide a *Map API*, accessible from a scene, that serves these operations through the STR tree index built at load time (Sec. 3.1), e.g., retrieving all lanes near the ego vehicle, as shown in the following.

```

from py123d.api import MapAPI, SceneAPI, SceneFilter, get_filtered_scenes
scene_filter = SceneFilter( # Mix datasets with different rigs and native rates.
    split_names=["av2-sensor_train", "nuscnescs_train", "wod-perception_train"],
    target_iteration_duration_s=0.5, # 2 Hz shared reference rate
    future_duration_s=4.0, history_duration_s=1.0, shuffle=True)
scene: SceneAPI = get_filtered_scenes(scene_filter, data_root=...)[0]
# 1. Sync access: ego / lidar at initial iteration.
ego = scene.get_ego_state_se3_at_iteration(iteration=0)
lidar = scene.get_lidar_at_iteration(iteration=0, lidar_id="lidar_top")
# 2. Async access: the nearest front-camera frame to the lidar sweep.
camera = scene.get_camera_at_timestamp(
    timestamp=lidar.timestamp_start, camera_id="pcam_f0", criteria="nearest")
# 3. Map access: query nearby lanes and crosswalks around ego.
map_api: MapAPI = scene.get_map_api()
nearby = map_api.get_map_objects_in_radius(
    point=ego.center_3d, radius=50.0, layers=["lane", "crosswalk"])

```

Visualization & Tools. We include an interactive 3D viewer based on Viser [71] (see Fig. 3), supporting point clouds, images, bounding boxes, and map elements, alongside matplotlib utilities for 2D visualizations such as bird’s-eye-view and camera overlay plots. A geometry utility library provides coordinate transformations, projection operations, and related primitives used throughout the framework and available to downstream code. Standalone examples, including a PyTorch dataset built on scenes and dataset conversion templates, are provided to lower the barrier to adoption.

4 Experiments

In this section, we use 123D’s standardized format to compare several established driving datasets. Our analysis has two aims. First, we provide a deeper understanding of the datasets themselves by analyzing differences in their annotations (Sec. 4.1) and pose and calibration quality (Sec. 4.2). Second, we demonstrate cross-dataset perception and simulation applications, by studying multi-view 3D object detection (Sec. 4.3) and reinforcement learning for planning (Sec. 4.4).

Datasets. Producing annotations, such as bounding boxes, is labor-intensive, and the resulting trade-off between label fidelity and scale divides existing driving datasets into three categories, as shown in Table 1: **(1) Manual labeling.** Trained annotators draw or review boxes from the sensor stack (often across multiple passes), providing high fidelity at considerable labor cost. Supported datasets in this category are nuScenes [6] (incl. 2Hz→10Hz bounding box interpolation), WOD-Perception [56], Argoverse 2 Sensor [66], PandaSet [67], and KITTI-360 [46], with durations ranging from 0.2 to 6.4

Table 1: Datasets. We compare scale (duration, driven distance, number of logs), sensor setup (number, sampling rate), and annotation availability (3D boxes, traffic light states, HD maps).

	Dataset	Year	Scale			Sensors [# / Hz]		Annotations [✓ / Hz]		
			Dur. [h]	Dist. [km]	Logs [#]	Cam.	Lidar	3D Box	Tls.	Map
Manual	nuScenes [6]	2020	5.6	100.9	1,000	6/12	1/20	✓/2	✗	✓
	WOD-Perc. [56]	2020	6.4	154.0	1,150	5/10	5/10	✓/10	✗	✓
	AV2-Sens. [66]	2021	4.4	87.5	1,000	9/20	2/10	✓/10	✗	✓
	PandaSet [67]	2021	0.2	8.3	103	6/10	2/10	✓/10	✗	✗
	KITTI-360 [46]	2022	2.7	73.7	9	4/10	1/10	✓/10	✗	✓
Auto-labeled	WOD-Mot. [21]	2021	574.1	10,323.5*	103,354	✗	✗	✓/10	✓/10	✓
	nuPlan [35]	2024	1,174.3	17,808.6	15,910	8/10 [†]	5/20 [†]	✓/20	✓/20	✓
	– mini		7.2	103.0	64					
	PAI-AV [51]	2025	1,707.0	69,265.7	307,332	7/30	1/10	✓/10	✗	✗
– NCore [53]	2026	6.3	167.6	1,147						
Synth.	CARLA [20]	2017	<i>var.</i>	<i>var.</i>	<i>var.</i>	<i>var.</i>	<i>var.</i>	✓	✓	✓
	– L3AD [50]	2026	7.3	138.7	789	6/10	2/10	✓/10	✓/10	✓

*Computed only from the non-overlapping 20 s training files. [†]Released for a 120 h subset; full coverage on mini.

hours. **(2) Auto-labeling.** Detection, tracking, and refinement pipelines generate boxes automatically from the sensor stack, covering thousands of hours of data at reduced fidelity. In this category, we include WOD-Motion [21], nuPlan [35], and PAI-AV [51]. For comparable duration and to remain within our storage budget, we limit experiments to the *mini* and *NCore* subsets of nuPlan and PAI-AV, respectively. We exclude WOD-Motion from experiments that require sensor data. **(3) Synthetic.** Simulators provide unlimited labeled data, inferred from the ground-truth state of the virtual driving environment. We provide a configurable collection pipeline for CARLA [20], based on the state-of-the-art expert policy LEAD [50]. To demonstrate this collection pipeline, we publish our L3AD dataset, which includes maps and roughly 7h of recordings that mirror the nuScenes sensor layout (see Fig. 3i), enabling the sim-to-real transfer study in our 3D object detection experiment (Sec. 4.3). Dataset-specific implementations are detailed in the supplementary material.

4.1 Cross-Dataset Annotation Analysis

We analyze the different annotation strategies between all nine datasets in terms of box ego distance, speed, and acceleration distributions, as shown in Fig. 4. For this, we summarize the original semantic labels to five categories: vehicle (e.g., car, bus, truck), person (e.g., pedestrian, rider), two-wheeler (e.g., bicycle, motorcycle), obstacles (e.g., traffic cone, barrier, sign), and other (e.g., train, animal). A complete summary of semantic labels can be found in the supplementary material.

Results. *Annotation range* varies widely: AV2-Sens., PandaSet, and PAI-AV stand out by labeling boxes ranging from 200 meters and more, while the remaining adopt narrower annotation ranges. Note that we apply configurable range limits in CARLA and KITTI-360 here, in order to avoid annotating city-wide assets on a per-timestamp basis. *Speed* shows an expected ordering, with vehicles fastest and two-wheelers second. The long high-speed vehicle tails in WOD-Perc., WOD-Mot., and PAI-AV reflect the highway driving present in those logs, whereas more urban datasets rarely exceed 20 m/s. Semantic ambiguities and label errors are particularly prevalent in the person class. For instance, AV2 and KITTI-360 apply separate bounding boxes for the rider and the two-wheeler, whereas WOD-Perc. annotates e-scooters as pedestrians. *Acceleration* most clearly shows the labeling-quality gap between regimes: auto-labeled datasets (WOD-Mot., nuPlan, PAI-AV) carry visibly wider acceleration tails across categories, caused by per-frame box jitter from their detection-and-tracking pipelines. Together, these differences underscore that working across heterogeneous datasets requires careful treatment of label conventions and quality. Since 123D preserves the original annotations as-is, we view re-annotation and open-vocabulary methods as an interesting application to explore.

4.2 Pose Accuracy & 3DGS Reconstruction

Beyond annotation quality, pose accuracy and sensor calibration are equally important for applications such as photorealistic sensor simulation and multi-sensor fusion. To check whether each dataset’s released poses and calibrations support photorealistic reconstruction, we run a per-dataset consistency

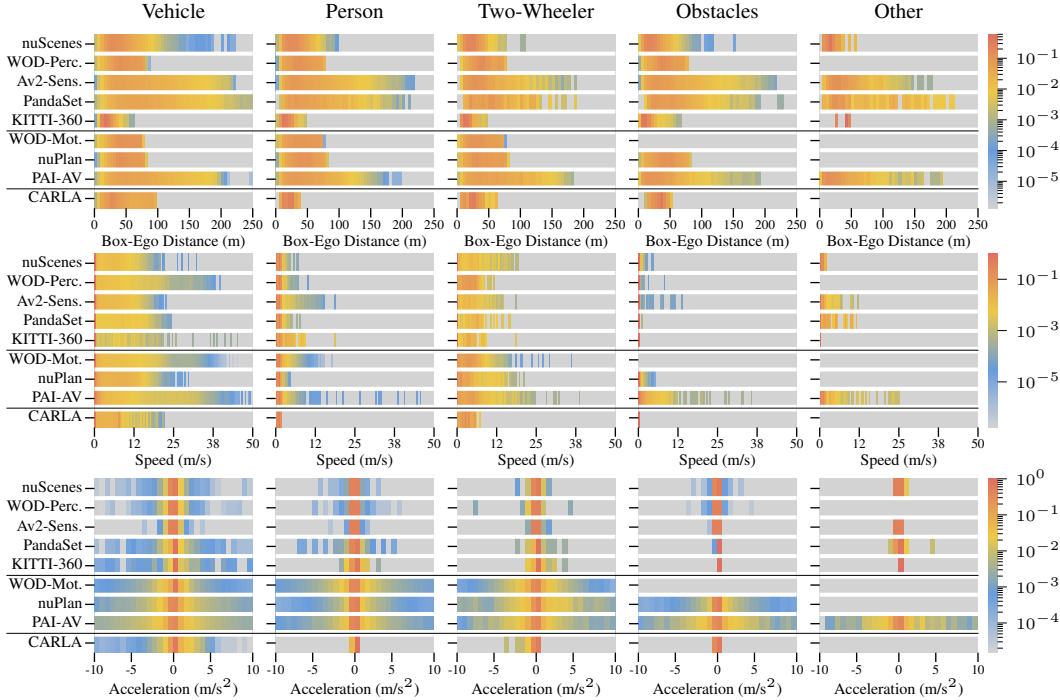


Figure 4: Annotation of bounding boxes. We compare ego distance, speed, and acceleration (rows) over different semantic categories, grouped into vehicle, person, two-wheeler, obstacles, and other miscellaneous classes (columns). The histograms show frequencies in the range of 0-1 on a log scale.

Table 2: FastGS reconstruction with and without lidar registration. We evaluate 100 scenes per dataset. Rendering metrics (PSNR, SSIM, LPIPS) are reported for models trained with original poses and with Kiss-ICP-registered poses [59], together with the translation and rotation disagreement between the datasets and registered poses. Per-column first, second, and third values are highlighted.

Dataset	Original Poses			Registered Poses			Registration Mismatch	
	PSNR \uparrow	SSIM \uparrow	LPIPS \downarrow	PSNR \uparrow	SSIM \uparrow	LPIPS \downarrow	\bar{t}_{err} (m) \downarrow	\bar{R}_{err} ($^\circ$) \downarrow
CARLA	31.97 \pm 3.45	0.889 \pm 0.05	0.184 \pm 0.08	29.53 \pm 4.38	0.833 \pm 0.08	0.224 \pm 0.07	0.844 \pm 2.20	0.96 \pm 3.53
Av2-Sens.	27.32 \pm 1.75	0.792 \pm 0.05	0.254 \pm 0.04	26.02 \pm 1.65	0.749 \pm 0.05	0.282 \pm 0.04	0.114 \pm 0.10	0.41 \pm 0.35
PAI-AV	26.66 \pm 2.29	0.826 \pm 0.07	0.212 \pm 0.05	26.22 \pm 2.28	0.812 \pm 0.07	0.223 \pm 0.05	0.158 \pm 0.11	0.31 \pm 0.32
WOD-Perc.	26.59 \pm 2.13	0.806 \pm 0.06	0.293 \pm 0.05	26.27 \pm 2.15	0.794 \pm 0.06	0.299 \pm 0.05	0.093 \pm 0.06	0.09 \pm 0.04
nuScenes	25.39 \pm 2.21	0.780 \pm 0.09	0.308 \pm 0.07	23.11 \pm 2.18	0.727 \pm 0.08	0.351 \pm 0.07	0.455 \pm 0.30	1.38 \pm 0.87
nuPlan	25.17 \pm 1.47	0.792 \pm 0.04	0.306 \pm 0.05	25.22 \pm 1.48	0.791 \pm 0.04	0.303 \pm 0.04	0.253 \pm 0.13	0.55 \pm 0.28
PandaSet	24.03 \pm 3.29	0.693 \pm 0.14	0.290 \pm 0.05	24.02 \pm 3.31	0.692 \pm 0.13	0.290 \pm 0.05	0.125 \pm 0.07	0.27 \pm 0.15
KITTI-360	19.92 \pm 1.75	0.684 \pm 0.05	0.346 \pm 0.04	19.36 \pm 1.69	0.665 \pm 0.05	0.360 \pm 0.04	0.174 \pm 0.09	0.40 \pm 0.26

check. Specifically, we create two reconstructions of each scene, one with the released poses and one with poses independently re-estimated by the Kiss-ICP lidar-based registration algorithm [59], to compare novel-view rendering quality. Importantly, this experiment is not a ranking of pose accuracy: neither pose source is ground truth, and rendering quality additionally reflects each dataset’s full sensor stack (lidar density, camera coverage, lighting, exposure). We select $N = 100$ scenes per dataset at 10 Hz over a fixed 7-second duration, choosing those whose ego-path length most closely matches the global median (~ 39 m) so that speed and distance are comparable across scenes. We generate per-frame semantic segmentation maps for all camera views using Mask2Former [13] and mask out dynamic semantic classes in image space so that reconstruction quality reflects only static scene geometry. For datasets with distorted images, we undistort the views using the provided intrinsic parameters. Using these inputs, we perform lidar point cloud stacking and FastGS reconstruction [54] (an efficient variant of 3DGS [36]) twice per scene, once with the released poses and once with the Kiss-ICP-estimated poses. We hold out every fourth camera rig capture as a test set to evaluate novel-view rendering quality. Further details are provided in the supplementary material.

Results. We summarize rendering quality and the disagreement between released and Kiss-ICP-estimated poses in Table 2. On most datasets, the released poses yield equal or slightly better rendering quality than the Kiss-ICP poses, indicating that the released calibrations are well-tuned

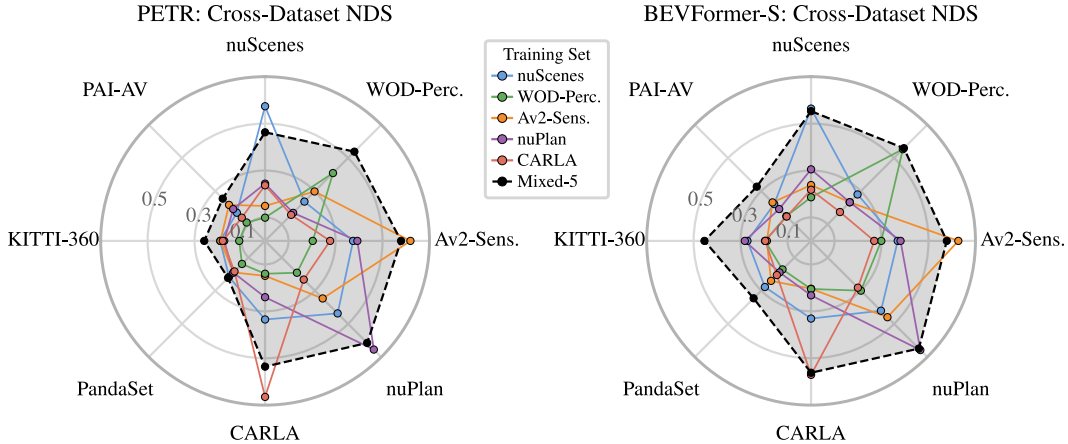


Figure 5: Multi-view 3D Object Detection. Per-dataset nuScenes detection score (NDS) for PETR [49] and BEVFormer-S [44] for *vehicle* detection. We evaluate on held-out validation splits of each dataset and train on nuScenes, WOD-Perc., Av2-Sens., nuPlan, CARLA, or a uniform mixture of these five (Mixed-5, dashed). PandaSet, KITTI-360, and PAI-AV are never seen during training.

for novel-view reconstruction; nuPlan is the only real dataset where Kiss-ICP gives a marginal improvement. The pose-disagreement column should be read as agreement between two pipelines rather than a pose-error estimate, since a large value can reflect either an issue in the released poses or a failure of Kiss-ICP itself. The largest disagreements occur on nuScenes (0.455 m) and CARLA (0.844 m), both of which use sparser 32-beam lidars whose returns may yield too few correspondences for reliable registration. Absolute rendering scores vary widely across datasets, but, as noted, reflect the sensor stack rather than a quality ordering. CARLA’s high scores are expected from a synthetic source with ground-truth poses, lower fidelity, and global shutters. KITTI-360’s lower scores arise due to the limited surround coverage (after undistorting the fisheye views) and as the lidar only projects onto the lower half of each image, leaving upper regions without point-based initialization.

4.3 Cross-Dataset Multi-View 3D Object Detection

Next, we study how well common camera-based 3D detectors generalize across sensor rigs and operating domains. We implement two representative non-temporal architectures, PETR [49] and BEVFormer-S [44], both with ResNet50 encoders [28], using the 123D interface. We restrict the evaluation to the *vehicle* class, the category with the least taxonomic ambiguity across datasets (Sec. 4.1), and to ground-truth boxes within a 50 m radius that are visible in the camera field of view and contain at least one lidar return. Following common practice in this setting [60, 9, 37], we report a modified nuScenes-detection-score (NDS) that excludes velocity and attribute errors. We train on nuScenes, WOD-Perc., AV2-Sens., nuPlan, and CARLA individually, and on a uniform mixture of all five (*Mixed-5*). To isolate data diversity from data volume, every training configuration uses a fixed budget of 30k frames (6k per dataset for *Mixed-5*). Further details are outlined in the supplementary.

Results. We summarize the cross-dataset transfer results for both detectors in Fig. 5. Single-dataset models retain 0.41–0.67 NDS in-domain but generally transfer poorly to other datasets (0.10–0.46 NDS). Transfer is asymmetric across sources: nuScenes is the most portable source relative to other single-dataset runs, while WOD-Perc. is the weakest, likely due to its limited 230° camera coverage seen during training. Despite using the nuScenes camera extrinsics, CARLA-trained models do not transfer preferentially to nuScenes (e.g., 0.24 for PETR), similar in performance to models trained on Av2-Sens. or nuPlan. This suggests that, for object detection, sim-to-real transfer is no easier than cross-rig transfer between real datasets, even when the simulator replicates the target rig.

Joint *Mixed-5* training closes most of these gaps at no extra training budget, approaching or exceeding single-dataset quality on most datasets in the mixture. BEVFormer-S benefits evenly (joint training closely matches single-dataset performance throughout), whereas PETR exhibits larger swings, such as gains on WOD-Perc. (0.41→0.54) but regressions on nuScenes (0.57→0.46).

Generalization to the three fully held-out datasets (PandaSet, KITTI-360, and PAI-AV) remains the hardest task. BEVFormer-S is consistently better here, exceeding PETR by 0.07–0.20 NDS,

suggesting that explicit BEV-grid representations transfer across rigs more robustly. Cross-rig generalization thus benefits from both training diversity and architectural inductive bias. However, the gaps remain substantial, leaving cross-rig generalization an open research problem that 123D now enables across eight heterogeneous real and synthetic datasets.

4.4 Reinforcement Learning for Planning

Data-driven simulators enable training and evaluation of policies with real-world maps and traffic states. However, they are commonly built for a single dataset [35, 27]. We demonstrate simulation across datasets by implementing a compatibility layer to PufferDrive [16], an optimized simulator for multi-agent reinforcement learning. We infer the route, a necessary input for reinforcement learning planners, for a subset of actors in a scene, covering the logged trajectory and beyond. We use the default policy and reward implemented in PufferDrive based on GIGAFLOW [17], which leverages self-play to control the selected actors during training. Each actor observes a vectorized view of lanes, boundaries, and other actors in the scene, together with 5 goal points to reach along the extracted route. We measure the success rate over agents as reaching the last point of the logged trajectory without off-road, red-light, or collision infractions. We conduct training and evaluation on WOD-Motion (9.1s with improved traffic lights [69]), nuPlan (20s), Av2-Sens. (15s, no traffic lights), and mixed training of these three (*Mixed-3*). As a held-out test environment, we evaluate on CARLA maps using randomly generated initial states of 40 actors in the scene, similar to [17].

Results. We summarize the results on held-out test scenes in Fig. 6. When evaluating WOD-Motion and nuPlan, we observe the best performance with in-domain trained models. Interestingly, policies trained with Av2-Sensor exhibit limited cross-domain generalization, but also underperform in-domain compared to nuPlan training, likely due to the absence of traffic lights and the simpler scenarios encountered during Av2-Sensor training. Cross-training jointly on all three real-world environments (*Mixed-3*) shows the highest success rates in the three in-domain environments. Importantly, the absolute gap to in-domain performance (i.e., WOD-Motion, nuPlan, or Av2-Sensor) on CARLA remains substantial, even for the *Mixed-3* approach which generalizes best. The results highlight the potential of cross-domain training and motivate further exploration in this research direction.

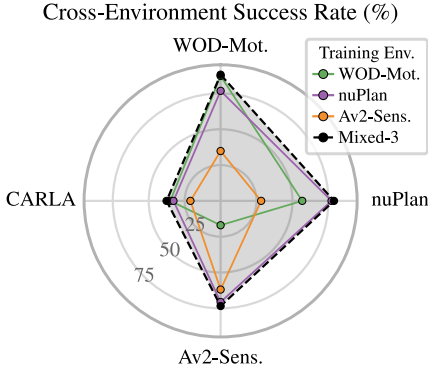


Figure 6: PufferDrive Planning [16].

5 Conclusion

In this paper, we present 123D, an open-source consolidation of diverse multi-modal driving datasets. It provides unified access to a wide range of sensor setups at an unprecedented scale. This, in turn, opens up new research questions that are not yet well explored. Our experiments demonstrate that cross-domain and vehicle transfer remains challenging for both perception and behavior tasks, and that simple data mixing reduces this gap to some extent. Going further, improved data mixing methods are an interesting avenue that has already proven crucial for training large language models [11, 26, 70]. To support this, we see particular promise in curating data through our API using foundation models for reasoning [62] and vision [8, 47], automatically aligning annotation guidelines [72, 73], and filtering specific scenarios [19]. By releasing 123D, we lower the barrier to pursuing these directions and leveraging large-scale, diverse data in autonomous driving.

Limitations. We identify three concrete limitations for future development. First, we currently focus on common sensor modalities widely available across datasets. Expanding support for additional sensors (e.g., radar [6, 51]) and annotations (e.g., semantic point clouds or images [67, 56, 6, 46]) remains a priority for the future. Second, 123D currently does not explicitly support web datasets or data streaming. However, the Apache Arrow IPC format provides features for cloud access [24] that we have preliminarily tested and hope to integrate in the future. Third, our supported datasets focus on standard vehicles. We aim to expand this scope to include trucks, mobile robots, and other platforms, and we invite community contributions to help broaden the coverage and utility of 123D.

Acknowledgments

This work was supported by ERC Starting Grant LEGO-3D (850533) and the DFG EXC number 2064/1 - project number 390727645. Daniel Dauner was supported by the German Federal Ministry for Economic Affairs and Energy within the project NXT GEN AI METHODS (19A23014S). This research used compute resources at the Tübingen Machine Learning Cloud, DFG FKZ INST 37/1057-1 FUGG as well as the Training Center for Machine Learning (TCML). We thank the International Max Planck Research School for Intelligent Systems (IMPRS-IS) for supporting Daniel Dauner.

References

- [1] Alex Aizman, Gavin Maltby, and Thomas Breuel. High performance i/o for large scale deep learning. In *2019 IEEE International Conference on Big Data (Big Data)*, pages 5965–5967. IEEE, 2019.
- [2] Kevin Black, Noah Brown, Danny Driess, Adnan Esmail, Michael Equi, Chelsea Finn, Niccolo Fusai, Lachy Groom, Karol Hausman, Brian Ichter, et al. π_0 : A vision-language-action flow model for general robot control. *arXiv.org*, 2024.
- [3] G. Bradski. The OpenCV Library. *Dr. Dobb’s Journal of Software Tools*, 2000.
- [4] Tom B. Brown, Benjamin Mann, Nick Ryder, Melanie Subbiah, Jared Kaplan, Prafulla Dhariwal, Arvind Neelakantan, Pranav Shyam, Girish Sastry, Amanda Askell, Sandhini Agarwal, Ariel Herbert-Voss, Gretchen Krueger, Tom Henighan, Rewon Child, Aditya Ramesh, Daniel M. Ziegler, Jeffrey Wu, Clemens Winter, Christopher Hesse, Mark Chen, Eric Sigler, Mateusz Litwin, Scott Gray, Benjamin Chess, Jack Clark, Christopher Berner, Sam McCandlish, Alec Radford, Ilya Sutskever, and Dario Amodei. Language models are few-shot learners. In *Advances in Neural Information Processing Systems (NeurIPS)*, 2020.
- [5] Remi Cadene, Simon Alibert, Alexander Soare, Quentin Gallouedec, Adil Zouitine, Steven Palma, Pepijn Kooijmans, Michel Aractingi, Mustafa Shukor, Dana Aubakirova, Martino Russi, Francesco Capuano, Caroline Pascal, Jade Choghari, Jess Moss, and Thomas Wolf. Lerobot: State-of-the-art machine learning for real-world robotics in pytorch. <https://github.com/huggingface/lerobot>, 2024.
- [6] Holger Caesar, Varun Bankiti, Alex H Lang, Sourabh Vora, Venice Erin Liong, Qiang Xu, Anush Krishnan, Yu Pan, Giancarlo Baldan, and Oscar Beijbom. nusenes: A multimodal dataset for autonomous driving. In *Proc. IEEE Conf. on Computer Vision and Pattern Recognition (CVPR)*, 2020.
- [7] Wei Cao, Marcel Hallgarten, Tianyu Li, Daniel Dauner, Xunjiang Gu, Caojun Wang, Yakov Miron, Marco Aiello, Hongyang Li, Igor Gilitschenski, Boris Ivanovic, Marco Pavone, Andreas Geiger, and Kashyap Chitta. Pseudo-simulation for autonomous driving. In *Proc. Conf. on Robot Learning (CoRL)*, 2025.
- [8] Nicolas Carion, Laura Gustafson, Yuan-Ting Hu, Shoubhik Debnath, Ronghang Hu, Didac Suris, Chaitanya Ryali, Kalyan Vasudev Alwala, Haitham Khedr, Andrew Huang, et al. Sam 3: Segment anything with concepts. *Proc. of the International Conf. on Learning Representations (ICLR)*, 2026.
- [9] Gyusam Chang, Jiwon Lee, Donghyun Kim, Jinkyu Kim, Dongwook Lee, Daehyun Ji, Sujin Jang, and Sangpil Kim. Unified domain generalization and adaptation for multi-view 3d object detection. *Advances in Neural Information Processing Systems (NeurIPS)*, 2024.
- [10] Ming-Fang Chang, John Lambert, Patsorn Sangkloy, Jagjeet Singh, Slawomir Bak, Andrew Hartnett, De Wang, Peter Carr, Simon Lucey, Deva Ramanan, et al. Argoverse: 3d tracking and forecasting with rich maps. In *Proc. IEEE Conf. on Computer Vision and Pattern Recognition (CVPR)*, 2019.
- [11] Mayee F Chen, Tyler Murray, David Heineman, Matt Jordan, Hannaneh Hajishirzi, Christopher Ré, Luca Soldaini, and Kyle Lo. Olmix: A framework for data mixing throughout lm development. *arXiv.org*, 2026.

- [12] Ziyu Chen, Jiawei Yang, Jiahui Huang, Riccardo de Lutio, Janick Martinez Esturo, Boris Ivanovic, Or Litany, Zan Gojcic, Sanja Fidler, Marco Pavone, et al. Omnire: Omni urban scene reconstruction. *Proc. of the International Conf. on Learning Representations (ICLR)*, 2025.
- [13] Bowen Cheng, Ishan Misra, Alexander G Schwing, Alexander Kirillov, and Rohit Girdhar. Masked-attention mask transformer for universal image segmentation. In *Proc. IEEE Conf. on Computer Vision and Pattern Recognition (CVPR)*, 2022.
- [14] OX-Embodiment Collaboration, Abby O’Neill, Abdul Rehman, Abhinav Gupta, Abhiram Maddukuri, Abhishek Gupta, Abhishek Padalkar, Abraham Lee, Acorn Pooley, Agrim Gupta, et al. Open x-embodiment: Robotic learning datasets and rt-x models. In *Proc. IEEE International Conf. on Robotics and Automation (ICRA)*, 2023.
- [15] MMDetection3D Contributors. MMDetection3D: OpenMMLab next-generation platform for general 3D object detection. <https://github.com/open-mmlab/mmdetection3d>, 2020.
- [16] Daphne Cornelisse*, Spencer Cheng*, Pragnay Mandavilli, Julian Hunt, Kevin Joseph, Waël Doulazmi, Valentin Charrat, Aditya Gupta, Joseph Suarez, and Eugene Vinitsky. PufferDrive: A fast and friendly driving simulator for training and evaluating RL agents, 2026. URL <https://github.com/Emerge-Lab/PufferDrive>.
- [17] Marco Cusumano-Towner, David Hafner, Alex Hertzberg, Brody Huval, Aleksei Petrenko, Eugene Vinitsky, Erik Wijmans, Taylor Killian, Stuart Bowers, Ozan Sener, et al. Robust autonomy emerges from self-play. *Proc. of the International Conf. on Machine learning (ICML)*, 2025.
- [18] Daniel Dauner, Marcel Hallgarten, Tianyu Li, Xinshuo Weng, Zhiyu Huang, Zetong Yang, Hongyang Li, Igor Gilitschenski, Boris Ivanovic, Marco Pavone, et al. Navsim: Data-driven non-reactive autonomous vehicle simulation and benchmarking. *Advances in Neural Information Processing Systems (NeurIPS)*, 2024.
- [19] Cainan Davidson, Deva Ramanan, and Neehar Peri. Refav: Towards planning-centric scenario mining. In *Proc. IEEE Conf. on Computer Vision and Pattern Recognition (CVPR)*, 2026.
- [20] Alexey Dosovitskiy, German Ros, Felipe Codevilla, Antonio Lopez, and Vladlen Koltun. CARLA: An open urban driving simulator. In *Proc. Conf. on Robot Learning (CoRL)*, 2017.
- [21] Scott Ettinger, Shuyang Cheng, Benjamin Caine, Chenxi Liu, Hang Zhao, Sabeek Pradhan, Yuning Chai, Ben Sapp, Charles R Qi, Yin Zhou, et al. Large scale interactive motion forecasting for autonomous driving: The waymo open motion dataset. In *Proc. of the IEEE International Conf. on Computer Vision (ICCV)*, 2021.
- [22] Lan Feng, Mohammadhossein Bahari, Kaouter Messaoud Ben Amor, Éloi Zablocki, Matthieu Cord, and Alexandre Alahi. Unitraj: A unified framework for scalable vehicle trajectory prediction. In *Proc. of the European Conf. on Computer Vision (ECCV)*, 2024.
- [23] Common Crawl Foundation. Common crawl. <https://commoncrawl.org>, 2026.
- [24] The Apache Software Foundation. Apache arrow. <https://github.com/apache/arrow>, 2026.
- [25] Andreas Geiger, Philip Lenz, and Raquel Urtasun. Are we ready for autonomous driving? The KITTI vision benchmark suite. In *Proc. IEEE Conf. on Computer Vision and Pattern Recognition (CVPR)*, 2012.
- [26] Aaron Grattafiori, Abhimanyu Dubey, Abhinav Jauhri, Abhinav Pandey, Abhishek Kadian, Ahmad Al-Dahle, Aiesha Letman, Akhil Mathur, Alan Schelten, Alex Vaughan, et al. The llama 3 herd of models. *arXiv.org*, 2024.
- [27] Cole Gulino, Justin Fu, Wenjie Luo, George Tucker, Eli Bronstein, Yiren Lu, Jean Harb, Xinlei Pan, Yan Wang, Xiangyu Chen, et al. Waymax: An accelerated, data-driven simulator for large-scale autonomous driving research. *Advances in Neural Information Processing Systems (NeurIPS)*, 2023.

- [28] Kaiming He, Xiangyu Zhang, Shaoqing Ren, and Jian Sun. Deep residual learning for image recognition. In *Proc. IEEE Conf. on Computer Vision and Pattern Recognition (CVPR)*, 2016.
- [29] John Houston, Guido Zuidhof, Luca Bergamini, Yawei Ye, Long Chen, Ashesh Jain, Sammy Omari, Vladimir Iglovikov, and Peter Ondruska. One thousand and one hours: Self-driving motion prediction dataset. In *Proc. Conf. on Robot Learning (CoRL)*, 2021.
- [30] Yihan Hu, Jiazhi Yang, Li Chen, Keyu Li, Chonghao Sima, Xizhou Zhu, Siqi Chai, Senyao Du, Tianwei Lin, Wenhai Wang, et al. Planning-oriented autonomous driving. In *Proc. IEEE Conf. on Computer Vision and Pattern Recognition (CVPR)*, 2023.
- [31] Open Geospatial Consortium Inc. Opendgis® implementation standard for geographic information - simple feature access - part 1: Common architecture. <https://www.ogc.org/standards/sfa>, 2011.
- [32] International Organization for Standardization. ISO 8855:2011(en) Road vehicles — Vehicle dynamics and road-holding ability — Vocabulary. <https://www.iso.org/obp/ui/en/#iso:std:iso:8855:>, 2011.
- [33] Boris Ivanovic, Guanyu Song, Igor Gilitschenski, and Marco Pavone. trajdata: A unified interface to multiple human trajectory datasets. In *Advances in Neural Information Processing Systems (NIPS)*, 2023.
- [34] Xiaosong Jia, Zhenjie Yang, Qifeng Li, Zhiyuan Zhang, and Junchi Yan. Bench2drive: Towards multi-ability benchmarking of closed-loop end-to-end autonomous driving. *Advances in Neural Information Processing Systems (NeurIPS)*, 2024.
- [35] Napat Karnchanachari, Dimitris Geromichalos, Kok Seang Tan, Nanxiang Li, Christopher Eriksen, Shakiba Yaghoubi, Noushin Mehdipour, Gianmarco Bernasconi, Whye Kit Fong, Yiluan Guo, et al. Towards learning-based planning: The nuPlan benchmark for real-world autonomous driving. In *Proc. IEEE International Conf. on Robotics and Automation (ICRA)*, 2024.
- [36] Bernhard Kerbl, Georgios Kopanas, Thomas Leimkühler, George Drettakis, et al. 3d gaussian splatting for real-time radiance field rendering. *ACM Trans. Graph.*, 42(4):139–1, 2023.
- [37] Zhaonian Kuang, Rui Ding, Haotian Wang, Xinhua Zheng, Meng Yang, and Gang Hua. Coin3d: Revisiting configuration-invariant multi-camera 3d object detection. *Proc. IEEE Conf. on Computer Vision and Pattern Recognition (CVPR)*, 2026.
- [38] Ted Lentsch, Santiago Montiel-Marín, Holger Caesar, and Dariu M Gavrilă. Terraseg: Self-supervised ground segmentation for any lidar. *Proc. IEEE Conf. on Computer Vision and Pattern Recognition (CVPR)*, 2026.
- [39] Scott T Leutenegger, Mario A Lopez, and Jeffrey Edgington. Str: A simple and efficient algorithm for r-tree packing. In *Proceedings 13th international conference on data engineering*, pages 497–506. IEEE, 1997.
- [40] Quentin Lhoest, Albert Villanova Del Moral, Yacine Jernite, Abhishek Thakur, Patrick Von Platen, Suraj Patil, Julien Chaumond, Mariama Drame, Julien Plu, Lewis Tunstall, et al. Datasets: A community library for natural language processing. In *Conference on Empirical Methods in Natural Language Processing (EMNLP)*, 2021.
- [41] Quanyi Li, Zhenghao Mark Peng, Lan Feng, Zhizheng Liu, Chenda Duan, Wenjie Mo, and Bolei Zhou. Scenarionet: Open-source platform for large-scale traffic scenario simulation and modeling. *Advances in Neural Information Processing Systems (NeurIPS)*, 2023.
- [42] Tianyu Li, Yihang Qiu, Zhenhua Wu, Carl Lindström, Peng Su, Matthias Nießner, and Hongyang Li. Mtgs: Multi-traversal gaussian splatting. *arXiv.org*, 2025.
- [43] Yueyuan Li, Songan Zhang, Mingyang Jiang, Xingyuan Chen, Jing Yang, Ye Qiang Qian, Chunxiang Wang, and Ming Yang. Tactics2d: A highly modular and extensible simulator for driving decision-making. *IEEE Transactions on Intelligent Vehicles (T-IV)*, 2024.

- [44] Zhiqi Li, Wenhai Wang, Hongyang Li, Enze Xie, Chonghao Sima, Tong Lu, Qiao Yu, and Jifeng Dai. Bevformer: learning bird’s-eye-view representation from lidar-camera via spatiotemporal transformers. *Proc. of the European Conf. on Computer Vision (ECCV)*, 2022.
- [45] Zhiqi Li, Zhiding Yu, Shiyi Lan, Jiahao Li, Jan Kautz, Tong Lu, and Jose M Alvarez. Is ego status all you need for open-loop end-to-end autonomous driving? In *Proc. IEEE Conf. on Computer Vision and Pattern Recognition (CVPR)*, 2024.
- [46] Yiyi Liao, Jun Xie, and Andreas Geiger. Kitti-360: A novel dataset and benchmarks for urban scene understanding in 2d and 3d. *IEEE Trans. on Pattern Analysis and Machine Intelligence (PAMI)*, 2022.
- [47] Haotong Lin, Sili Chen, Junhao Liew, Donny Y Chen, Zhenyu Li, Guang Shi, Jiashi Feng, and Bingyi Kang. Depth anything 3: Recovering the visual space from any views. *arXiv.org*, 2025.
- [48] Mingyu Liu, Ekim Yurtsever, Jonathan Fossaert, Xingcheng Zhou, Walter Zimmer, Yuning Cui, Bare Luka Zagar, and Alois C Knoll. A survey on autonomous driving datasets: Statistics, annotation quality, and a future outlook. *IEEE Transactions on Intelligent Vehicles (T-IV)*, 2024.
- [49] Yingfei Liu, Tiancai Wang, Xiangyu Zhang, and Jian Sun. Petr: Position embedding transformation for multi-view 3d object detection. In *Proc. of the European Conf. on Computer Vision (ECCV)*, 2022.
- [50] Long Nguyen, Micha Fauth, Bernhard Jaeger, Daniel Dauner, Maximilian Igl, Andreas Geiger, and Kashyap Chitta. Lead: Minimizing learner-expert asymmetry in end-to-end driving. *Proc. IEEE Conf. on Computer Vision and Pattern Recognition (CVPR)*, 2026.
- [51] NVIDIA. PhysicalAI-Autonomous-Vehicles. <https://huggingface.co/datasets/nvidia/PhysicalAI-Autonomous-Vehicles>, 2025. Hugging Face dataset.
- [52] NVIDIA. NVIDIA DRIVE Hyperion: L4-Ready autonomous vehicle platform. <https://www.nvidia.com/en-us/solutions/autonomous-vehicles/drive-hyperion/>, 2026. NVIDIA product page.
- [53] NVIDIA. PhysicalAI-Autonomous-Vehicles-NCORE. <https://huggingface.co/datasets/nvidia/PhysicalAI-Autonomous-Vehicles-NCORE>, 2026. Hugging Face dataset.
- [54] Shiwei Ren, Tianci Wen, Yongchun Fang, and Biao Lu. Fastgs: Training 3d gaussian splatting in 100 seconds. *Proc. IEEE Conf. on Computer Vision and Pattern Recognition (CVPR)*, 2026.
- [55] Chonghao Sima, Katrin Renz, Kashyap Chitta, Li Chen, Hanxue Zhang, Chengen Xie, Jens Beißwenger, Ping Luo, Andreas Geiger, and Hongyang Li. Drivelm: Driving with graph visual question answering. In *Proc. of the European Conf. on Computer Vision (ECCV)*, 2024.
- [56] Pei Sun, Henrik Kretschmar, Xerxes Dotiwalla, Aurelien Chouard, Vijaysai Patnaik, Paul Tsui, James Guo, Yin Zhou, Yuning Chai, Benjamin Caine, et al. Scalability in perception for autonomous driving: Waymo open dataset. In *Proc. IEEE Conf. on Computer Vision and Pattern Recognition (CVPR)*, 2020.
- [57] OpenPCDet Development Team. Openpcdet: An open-source toolbox for 3d object detection from point clouds. <https://github.com/open-mmlab/OpenPCDet>, 2020.
- [58] Adam Tonderski, Carl Lindström, Georg Hess, William Ljungbergh, Lennart Svensson, and Christoffer Petersson. Neurad: Neural rendering for autonomous driving. In *Proc. IEEE Conf. on Computer Vision and Pattern Recognition (CVPR)*, 2024.
- [59] Ignacio Vizzo, Tiziano Guadagnino, Benedikt Mersch, Louis Wiesmann, Jens Behley, and Cyrill Stachniss. Kiss-icp: In defense of point-to-point icp—simple, accurate, and robust registration if done the right way. *IEEE Robotics and Automation Letters (RA-L)*, 8(2):1029–1036, 2023.
- [60] Shuo Wang, Xinhai Zhao, Hai-Ming Xu, Zehui Chen, Dameng Yu, Jiahao Chang, Zhen Yang, and Feng Zhao. Towards domain generalization for multi-view 3d object detection in bird-eye-view. *Proc. IEEE Conf. on Computer Vision and Pattern Recognition (CVPR)*, 2023.

- [61] Yan Wang, Xiangyu Chen, Yurong You, Li Erran Li, Bharath Hariharan, Mark Campbell, Kilian Q Weinberger, and Wei-Lun Chao. Train in germany, test in the usa: Making 3d object detectors generalize. In *Proc. IEEE Conf. on Computer Vision and Pattern Recognition (CVPR)*, 2020.
- [62] Yan Wang, Wenjie Luo, Junjie Bai, Yulong Cao, Tong Che, Ke Chen, Yuxiao Chen, Jenna Diamond, Yifan Ding, Wenhao Ding, et al. Alpamayo-r1: Bridging reasoning and action prediction for generalizable autonomous driving in the long tail. *arXiv.org*, 2025.
- [63] Waymo. Safe, routine, ready: Autonomous driving in five new cities. <https://waymo.com/blog/2025/11/safe-routine-ready-autonomous-driving-in-new-cities/>, 2025. Waymo blog post.
- [64] Waymo. Beginning fully autonomous operations with the 6th-generation Waymo driver. <https://waymo.com/blog/2026/02/ro-on-6th-gen-waymo-driver/>, 2026. Waymo blog post.
- [65] Wayve. Crossing the pond and beyond: Generalizable AI driving for global deployment. <https://wayve.ai/thinking/multi-country-generalization/>, 2025. Wayve blog post.
- [66] Benjamin Wilson, William Qi, Tanmay Agarwal, John Lambert, Jagjeet Singh, Siddhesh Khandelwal, Bowen Pan, Ratnesh Kumar, Andrew Hartnett, Jhony Kaesemodel Pontes, et al. Argoverse 2: Next generation datasets for self-driving perception and forecasting. *Advances in Neural Information Processing Systems (NeurIPS)*, 2021.
- [67] Pengchuan Xiao, Zhenlei Shao, Steven Hao, Zishuo Zhang, Xiaolin Chai, Judy Jiao, Zesong Li, Jian Wu, Kai Sun, Kun Jiang, et al. Pandaset: Advanced sensor suite dataset for autonomous driving. In *Proc. IEEE Conf. on Intelligent Transportation Systems (ITSC)*. IEEE, 2021.
- [68] Runsheng Xu, Hubert Lin, Wonseok Jeon, Hao Feng, Yuliang Zou, Liting Sun, John Gorman, Ekaterina Tolstaya, Sarah Tang, Brandyn White, et al. Wod-e2e: Waymo open dataset for end-to-end driving in challenging long-tail scenarios. *arXiv.org*, 2025.
- [69] Xintao Yan, Erdao Liang, Jiawei Wang, Haojie Zhu, and Henry X Liu. Improving traffic signal data quality for the waymo open motion dataset. *Transportation Research Part C: Emerging Technologies*, 183:105476, 2026.
- [70] An Yang, Baosong Yang, Beichen Zhang, Binyuan Hui, Bo Zheng, Bowen Yu, Chengyuan Li, Dayiheng Liu, Fei Huang, Haoran Wei, Huan Lin, Jian Yang, Jianhong Tu, et al. Qwen2.5 technical report. *arXiv.org*, 2024.
- [71] Brent Yi, Chung Min Kim, Justin Kerr, Gina Wu, Rebecca Feng, Anthony Zhang, Jonas Kulhanek, Hongsuk Choi, Yi Ma, Matthew Tancik, et al. Viser: Imperative, web-based 3d visualization in python. *arXiv.org*, 2025.
- [72] Xiangyun Zhao, Samuel Schuster, Gaurav Sharma, Yi-Hsuan Tsai, Manmohan Chandraker, and Ying Wu. Object detection with a unified label space from multiple datasets. In *Proc. of the European Conf. on Computer Vision (ECCV)*, 2020.
- [73] Xingyi Zhou, Vladlen Koltun, and Philipp Krähenbühl. Simple multi-dataset detection. In *Proc. IEEE Conf. on Computer Vision and Pattern Recognition (CVPR)*, 2022.